

## ORIGINAL ARTICLE

# Artificial intelligence aided design of film cooling scheme on turbine guide vane



Dike Li, Lu Qiu, Kaihang Tao, Jianqin Zhu\*

National Key Laboratory of Science and Technology on Aero-Engine Aero-thermodynamics, School of Energy and Power Engineering, Beihang University, Beijing, 100191, China

Received 8 August 2020; accepted 4 October 2020

Available online 9 December 2020

**KEYWORDS**

Film cooling;  
Machine learning;  
Fast prediction;  
Massive simulation automation;  
Turbine guide vane

**Abstract** In recent years, artificial intelligence (AI) technologies have been widely applied in many different fields including in the design, maintenance, and control of aero-engines. The air-cooled turbine vane is one of the most complex components in aero-engine design. Therefore, it is interesting to adopt the existing AI technologies in the design of the cooling passages. Given that the application of AI relies on a large amount of data, the primary task of this paper is to realize massive simulation automation in order to generate data for machine learning. It includes the parameterized three-dimensional (3-D) geometrical modeling, automatic meshing and computational fluid dynamics (CFD) batch automatic simulation of different film cooling structures through customized developments of UG, ICEM and Fluent. It is demonstrated that the trained artificial neural network (ANN) can predict the cooling effectiveness on the external surface of the turbine vane. The results also show that the design of the ANN architecture and the hyper-parameters have an impact on the prediction precision of the trained model. Using this established method, a multi-output model is constructed based on which a simple tool can be developed. It is able to make an instantaneous prediction of the temperature distribution along the vane surface once the arrangements of the film holes are adjusted.

© 2020 Beihang University. Production and hosting by Elsevier B.V. on behalf of KeAi. This is an open access article under the CC BY-NC-ND license (<http://creativecommons.org/licenses/by-nc-nd/4.0/>).

\*Corresponding author.

E-mail address: [zhujianqin@buaa.edu.cn](mailto:zhujianqin@buaa.edu.cn) (Jianqin Zhu).

Peer review under responsibility of Beihang University.



Production and Hosting by Elsevier on behalf of KeAi

<https://doi.org/10.1016/j.jppr.2020.10.001>

2212-540X/© 2020 Beihang University. Production and hosting by Elsevier B.V. on behalf of KeAi. This is an open access article under the CC BY-NC-ND license (<http://creativecommons.org/licenses/by-nc-nd/4.0/>).

## 1. Introduction

Film cooling is an effective method to protect the turbine vanes and blades from damage due to the high turbine inlet temperature in modern advanced gas turbines. There are hundreds of film holes arranged on the external surface of a typical turbine vane, which elevates the difficulty of the optimization of the hole arrangements due to the massive number of geometrical parameters, such as the diameter, location, and inclination of the holes. Meanwhile, with the continuous burst of data and computer development, artificial intelligence (AI) technology has been applied in various industries in order to improve the efficiency. In the field of aero-engines, AI technologies have already been adopted in many different applications, such as compressor tip clearance design [1], engine monitor [2], engine control [3], fault detection and isolation [4]. Due to its high efficiency and intelligence, it plays an increasingly important role.

In the film cooling design on the turbine vane, experimental research and numerical simulation are two basic methods. So far, many scholars or engineering designers have used these methods to carry out researches on the film cooling. However, the study of film cooling at different operating conditions with various geometrical configurations implies an excessive economical and computational cost. In order to reduce such costs, AI technologies are employed to improve the cooling effectiveness and reduce the area-averaged heat transfer [5], optimize the multi-disciplinary design of the internal and external cooling structures [6], improve the prediction of turbulent heat transfer [7], etc. For example, Wang et al. [8,9] conducted the investigations on the shape optimization of a laidback fan-shaped film cooling hole with the least square support vector machine (LS-SVM). In the numerical simulation of a novel shaped film-cooling hole, the radial basis neural network model is constructed and the sequential quadratic programming is used to optimize the hole shape [10]. Qin et al. [11] applied the Back Propagation (BP) neural network to predict the adiabatic film cooling effectiveness with multi geometry and flow parameters while some other researchers used the group method of data handling (GMDH)-type neural networks [12,13]. It is worth noting that most of the researches were carried out on the plate or part of a vane, or other simple models, mainly for the specific heat transfer mechanism, thus lacking of the cooling experience with complete and complicated vane models.

AI technology is driven by data. Therefore, the very first obstacle in front of implementing AI into the design of cooling scheme of turbine is the generation of sufficient and suitable data for the training. To this end, computational fluid dynamics (CFD) [14] was commonly employed to generate the raw data. The CFD method itself could also be optimized by machine learning [15] where the classical Reynolds-averaged Navier-Stokes (RANS) turbulence models were improved with AI methods. The essence of machine learning is generating the implicit correlations

between the inputs and outputs. Regarding the film cooling, the outputs could be area-averaged film cooling effectiveness [16], the film cooling heat transfer coefficient [17], the temperature distribution [18], etc. and the design variable inputs included hole diameter [19], compound angle [20], hole pitch [21], column pitch [22], blowing ratio [17], etc. In detail, Payandehdoost et al. [17] predicted the film cooling heat transfer coefficient with respect to the blowing ratio, the total temperature of a coolant jet, the injection angle and the location of injection slots using neural networks. Lee et al. [14] evaluated the effects of the ejection and lateral ejection angles of the double-jet film cooling holes. In Ayoubi et al. [20]'s work, three geometric variables defining the hole shape were studied: the conical expansion angle, the compound angle and the length to diameter ratio of the non-diffused portion of the hole. Although great many parameters and objective functions have been investigated in the existing open literature, most of them are separated and aimed at the impact on a local scale. It is still lack of an efficient tool to quickly predict the overall temperature or cooling effectiveness distribution based on the global parameters of the vane, which is essential to the designers.

From these studies, it can be seen that the use of machine learning methods to assist in the design of film cooling structure is promising. However, there are still many shortcomings. Most of the researches were working on simple geometries, such as a flat or a small fraction of the vane surface, and were limited to narrow ranges of parameters. It is unclear whether the AI could make a good prediction of the film cooling effectiveness distribution on the surface of a complete 3-D turbine guide vane, with all the geometrical parameters of the film cooling structure as the inputs. In addition, what kind of artificial neural network (ANN) can achieve higher prediction accuracy also needs more trials. Therefore, the goal of this paper is to establish a machine learning method under the data shortage condition in the initial stage of film cooling structure design and obtain a high-speed and high-precision cooling effectiveness prediction model according to the geometrical parameters of the film cooling schemes on an entire 3-D vane, and explore the ANN with the best performance in this process.

## 2. Methods

### 2.1. The main ideas of AI aided design for turbine vane cooling

As aforementioned, in order to develop the core of the AI aided design method for the film cooling arrangements on a turbine guide vane, the generation of the data is not only important but also necessary. The developed tool is expected to be able to instantaneously predict the variations of film cooling effectiveness along the vane surface with the parametrical input of the hole arrangements. Therefore, the first step of current work is to generate data to train the AI model. The desired data should be corresponding film

cooling effectiveness distributions under different film hole schemes. Aiming to improve the efficiency of the process, a massive simulation automation platform is developed. Then, different input parameters and objective variables are extracted from the 3-D flow and temperature fields of the simulation results to train the ANN and conducts the result tests and evaluations. Finally, a fast and high-accuracy prediction tool based on the trained ANN is developed in order to realize the AI aided design for film cooling structure of turbine guide vane. The flow chart of the AI aided design of film cooling schemes under the data shortage condition introduced in this article is shown in Figure 1.

## 2.2. Massive simulation automation

As mentioned, AI technology is driven by data and this paper attempts to construct the proper ANN to establish a connection between geometrical parameters of film cooling structure and cooling effectiveness, thus the data applicable to this scenario is extremely essential and needed, which is the foundation to this all. In this work, the numerical simulation method is used and the massive simulation automation that consists of parameterized 3-D geometrical modeling, automatic meshing and CFD batch automatic setup and simulation should be realized for labor saving.

### 2.2.1. Parameterized 3-D geometrical modeling

In the 3-D modeling, the commercial software NX 10.0 (UG) is used and NX OPEN is determined as the customized development method with the coding platform selected as Visual Studio 2012. A slice of a turbine guide vane, with a height of 18 mm, is cut and modeled. The wall thickness is fixed at 1 mm and all the film holes are cylinder. The cooling structure inside the vane is not considered and the entire cavity is set as a coolant passage. The top of the vane

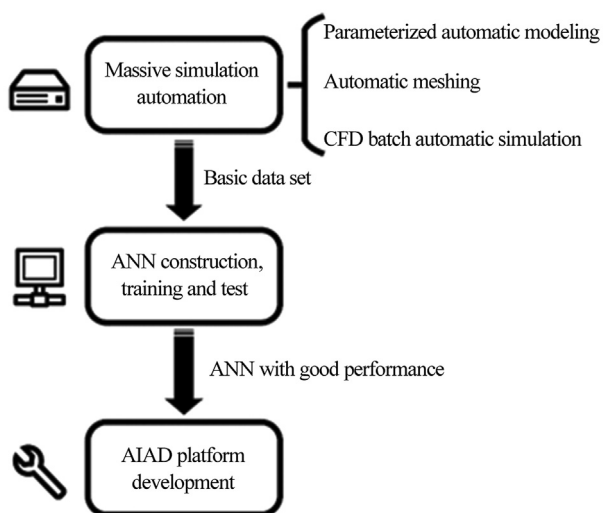


**Figure 1** The flow chart of the AI aided design of film cooling schemes under the data shortage condition in the initial stage of vane design.

is closed and the coolant gets in from the bottom and then enters the high temperature mainstream from the film holes, thereby forming a cooling film on the vane surface. The user enters the coordinates of two points inside and outside the vane, and the program automatically calculates the location and inclination of the hole. Then, according to the input diameter and hole pitch, the drilling of one column is automatically completed and all the geometrical parameters are displayed. After repeating this operation, the entire 3-D geometries with different arrangements of film holes can be easily generated.

In order to run the CFD simulation, the model of the corresponding flow field should be established, which is also fixed in all the cases in current work. The length of the flow field is 90 mm, the width is 54 mm and the height is 18 mm that is equal to the vane height. The entire fluid domain is set as computational domain and the geometry of it is exported for meshing. The geometry model of the guide vane and the computational domain with the flow field is shown in Figure 2.

### 2.2.2. Automatic meshing

Before the numerical simulation, meshing is essential and the meshes of all the models are generated in ICEM CFD 17.1. Because the high temperature mainstream in the vicinity of the vane surface interacts strongly with the coolant injection, the heat transfer is more intense and the flow field is more complicated. Therefore, the outer surface of the vane needs mesh encryption. Some cooling passages with small hole diameter as well as the corresponding inner surfaces also need mesh encryption. In addition, all cases contain 10 layers of boundary layer grids, and the height of the initial layer is 0.002 mm with a growing ratio of 1.1. The global element scale factor and max element are set at 1.0 and 2.0 respectively, while the local max element ranges from 0.08 to 0.2 for different film hole schemes.

Similarly, the customized development of ICEM is also performed in order to automate the meshing process, which is realized by reading the function script files in the replay scripts module. The script file code is written based on the TCL (tool command language) scripting language. A simple example with relatively sparser grids of the generated mesh is shown in Figure 3, which aims to show the general state of the mesh.

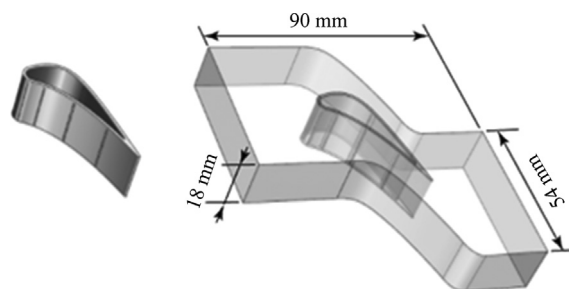


**Figure 2** The geometry model of the guide vane and the computational domain with the flow field.

2.2.3. CFD batch automatic setup and simulation

Through the parameterized modeling and automatic meshing described above, a large number of computational domain grids can be quickly obtained. Then ANSYS Fluent 17.1 software is adopted to numerically simulate the 3-D flow fields and temperature fields of all models. As the current work is still in the exploration and verification stage, there are no clear restrictions and requirements on the boundary conditions. However, it is notable that the flow conditions and aerodynamic shape of the guide vane are all fixed in all of the cases. The simulation method and settings refer to the existing published literatures [23], and they were all verified by experiments. The specific computation conditions are set as shown in Table 1. The problem was modeled by steady RANS and the shear stress transport (SST)  $k-\omega$  model was used as the turbulence model. The SST model has higher calculation accuracy and reliability for complex flow conditions, and is widely used in the numerical simulation of vanes in engineering. Liu et al. [24] used ANSYS CFX 11.0 software to verify the four turbulence models of standard  $k-\epsilon$  model, RNG  $k-\epsilon$  model,

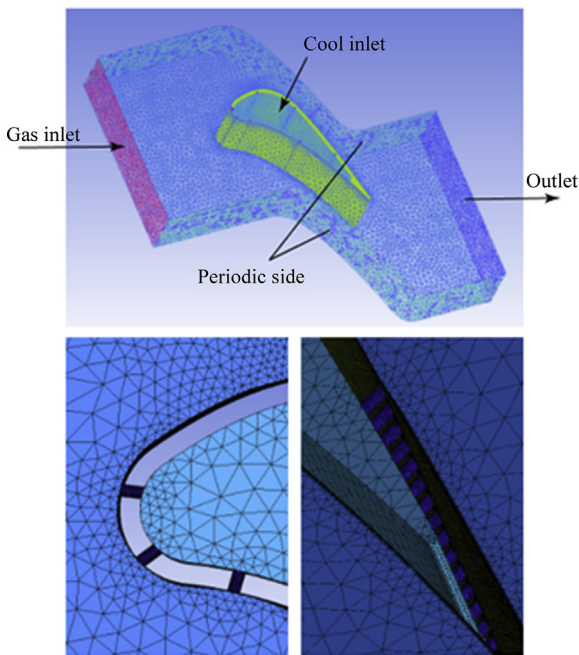


Figure 3 One of the grids of the computational domain obtained by automatic meshing.

Table 1 The computation method and boundary conditions setting.

Computation domain	Entire fluid domain
Fluid type	Ideal compressible gas
Turbulence model	$k-\omega$ SST
Mainstream speed inlet	10 m/s, 1300 K
Coolant mass flow inlet	0.0002 kg/s, 670 K
Pressure outlet	1 atm
Cascade sides	Periodic boundary
Other walls	No slip adiabatic wall

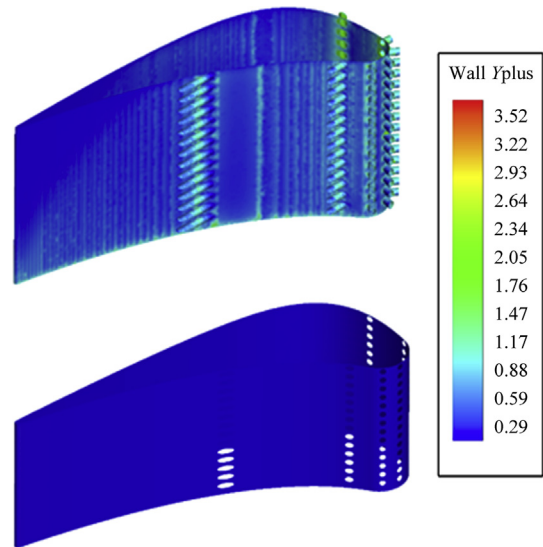


Figure 4 The wall  $Y^+$  distributions at the vane boundaries for one of the cases obtained by batch automatic setup and simulation.

standard  $k-\omega$  model and SST  $k-\omega$  model for numerical simulation of impingement cooling and film cooling, respectively. A comparative study was made and compared with the experimental data of Metzger et al. [25] and Maikell et al. [26] and it showed that the SST  $k-\omega$  model had the smallest error relative to the experimental data, which was 5.85%. The solver type was pressure-based and the scheme of pressure-velocity coupling was determined as SIMPLE to generate solutions. The second-order upwind differencing was used for spatial discretization, which has a higher precision. For all computations, iterations were continued until all residuals for all equations plateau to ensure convergence to steady state has been reached.

The purpose of the massive simulation automation is to provide sufficient data for ANN training, so it is necessary to carry out numerical simulations for many different cases. The massive simulation automation in Fluent is achieved by the batch program. Based on a case with complete setups of model, boundary and solver, the batch program could replace the mesh, run the calculation and save the data automatically. It is worth noting that the  $y^+$  of all cases is ensured to be approximately equal to 1 or less, in order to meet the requirements of the SST  $k-\omega$  turbulence model for the meshes. Figure 4 shows the  $Y^+$  distributions at the vane boundaries for one of the cases in current work.

2.2.4. Preliminary construction of the datasets

Considering the saving of computing resources and the exploratory nature of current work, a basic data set with 90 models has been initially constructed. Each model has 7 columns of film holes and each column has 7 parameters: axial ratio, radio ratio, centerline vector  $X, Y, Z$ , hole diameter and hole pitch. Thus, there are 49 geometrical parameters to describe the arrangements of the film holes.

Those parameters should be the input layer of the ANN and the corresponding film cooling effectiveness is the output layer. However, the amount of the input parameters is too large to be handled by the ANN due to current relatively small data size. It could be better to reduce the dimension. Therefore, all of the models are given a fixed radial ratio of the location holes and the center line vector  $Z$ . In addition, the diameter of the holes and the hole pitch in each model are also the same. As a result, the number of global geometrical parameters can be reduced from 49 to 23. Table 2 shows the specific parameters of the film holes and the 3-D temperature fields information obtained by numerical simulation. It is composed of 9 different combinations of axial locations, center line vector  $X$  and  $Y$ , 5 different hole diameters and 2 different hole pitches, and these variable parameters are all randomly selected. It is worth emphasizing that the flow conditions and aerodynamic shape of the turbine guide vane are all fixed in all of the cases, with only film cooling schemes varying from case to case.

### 2.3. ANN construction

With the data set generated by the process explained above, an ANN can then be constructed to establish the correlation between geometrical parameters of film holes and cooling effectiveness, which is the core of this paper. The entire process was completed on MATLAB 2016. At present, many machine learning frameworks based on Python are quite mature and excellent, such as TensorFlow and Pytorch. But it is recognized that they are more suitable for engineering projects, that is, large-scale industrial applications. On the contrary, the advantage of MATLAB is that it is easy to carry out small-scale algorithm tests and instance operations, so it is more popular and commonly used in academia. Thus, MATLAB is utilized as a computing platform in current work. The ANN framework was imported through a function called 'newff' and the ANN constructed here was a BP neural network based on Levenberg-Marquardt (L-M) algorithm, which is classic and powerful. The data involved was normalized by 'mapminmax'

**Table 2** The information contained in the basic data set.

Number of models	90
Number of columns for each model	7
Geometrical parameters of film holes	For each column: Axial ratio, center line vector $X$ , $Y$ , hole diameter, hole pitch, Radial ratio (location) = 0.0676, $Z = 0$ .
Numerical simulation results	Area average temperature of the vane surface, the leading edge. The pressure side, the suction side. Line average temperature. Line average cooling efficiency. ...

function and the training parameters were set by 'net.trainParam.' function.

The ANN is essentially a high-dimensional nonlinear mapping from the input to output and is generally divided into three parts: input layer, hidden layer and output layer. Obviously, the input and output layers are the geometrical parameters of film holes and the cooling effectiveness respectively. However, which combination of the input and output has a better performance in the ANN still needs more practical tests. For the determination of hidden layers and nodes, it is essential to get a rough estimation according to some empirical formulas and then conduct more trials within a reasonable range. Nodes between different layers are connected to each other by weights, biases and activation functions (also known as transfer functions) that can be adjusted at the start of the training process.

It is worth noting that the initial weights and biases can be optimized by introducing the genetic algorithm (GA). The existing research shows that the GA based neural network training could perform better than back propagation or its faster variants. Hiroaki Kitano was roughly the first to attempt to systematically evaluate the efficiency of GA-BP method [27]. The GA is a global parallel and random search optimization method. The principle is to simulate the biological genetic mechanism of nature and the biological evolution rule of "survival of the fittest". The environmental adaptability of each generation is constantly improving. In the ANN optimization, the basic idea is to treat the initial weights and biases as individuals of each generation and the corresponding cost function is taken as the fitness value. Through the genetic mechanism of selection, crossover and mutation, the best individual is found generation by generation, thus determining the optimal initial weights and biases of the network when the population evolves to the highest level. Wang et al. [28] computed the area-averaged film cooling effectiveness for a gas turbine guide vane using the BP neural networks with the weights and biases of the networks optimized by the GAs. In current work, the population of each generation contains 50 individuals, given 100 generations.

The following indexes are calculated to evaluate the performance of the constructed ANN.

Mean square error (MSE):

$$E_1 = \frac{1}{n} \sum_1^n |K_D - K_P|^2 \quad (1)$$

Mean relative error (MRE):

$$E_2 = \frac{1}{n} \sum_1^n (|K_D - K_P| / K_D) \quad (2)$$

Fitting determination coefficient:

$$R^2 = \frac{[\sum_n (K_D - \bar{K}_D)(K_P - \bar{K}_P)]^2}{[\sum_n (K_D - \bar{K}_D)^2][\sum_n (K_P - \bar{K}_P)^2]} \quad (3)$$

where  $K_D$  and  $K_P$  are the network expected output and actual output of one sample respectively,  $n$  is the number of test samples. Here, the MSE is used as training performance, that is, to tell the machine when to stop training. The MRE and the determination coefficient are calculated and presented to the user to compare the quality of the constructed ANN.

### 3. Results and discussions

#### 3.1. Design of ANN

##### 3.1.1. Effect of ANN inputs and outputs selection

As aforementioned, the preliminary constructed data set contains 90 models that will be used to train and test the ANN. With different inputs and outputs, the ANNs were constructed, trained and tested on MATLAB platform. It should be noted that the parameters of the hot gas and cooling air are identical whereas the arrangements of the film holes are different from case to case. The data set was randomly divided into two parts in each run of the program, 75% as the training set and 25% as the test set. The number of hidden layers was set to one. The number of nodes in the hidden layer was roughly calculated by empirical formulas and the best one was selected. The activation function was ‘tansig’ between the input layer and the hidden layer and was ‘purelin’ between the hidden layer and the output layer. Table 3 shows different architectures of the ANN with various combinations of the input layer, output layer and hidden layer.

Since the training set and test set are randomly divided, the results of each experiment have some differences. However, it is notable that the test results of the two groups (1, 2) with the average temperature of the surface output are extremely similar and the results of the three groups (3, 4, 5) with the average temperature of the line output are also very close to each other. The results of one of these experiments are shown in Figure 5. The left column shows the results of a single run on the test set, and the middle and right columns show the determination coefficients and MREs for 100 runs,

respectively. The average values of the 100 runs are also marked in the Figures. As shown in Figure 5(a), the prediction precision of mean temperature across the external surface of entire guide vane and leading edge is relatively low. The average determination coefficient  $R^2$  of 100 runs is only in the range from 0.2 to 0.4, indicating that the correlation between the inputs and outputs is weak. The reason can be inferred that the temperature difference across the blade surface is prominent whereas the simple average of the surface temperature could bury the local physical parameters, which would be strong related to the arrangements of the film holes. Therefore, it can be concluded that it is not reasonable to directly use the overall mean temperature or mean cooling efficiency of the surface as an output parameter.

Once the parameter in the output layer is local mean temperature rather than overall mean temperature, as shown in Figure 5(b), the prediction of ANN is more accurate. In most of the cases, the determination coefficient is between 0.8 and 0.95, and the relative error in predicting temperature is less than 5%, indicating that the output parameter is strongly connected with the inputs. Moreover, as shown in Figure 5(c), the local parameter of the film cooling efficiency is set to be the output layer. The results show that the prediction is relatively good and the mean determination coefficient is around 0.84. Therefore, it can be concluded that choosing local parameters is better than overall parameters to construct the output layer.

Unlike the output layer, the results do not change too much with different structures of the input layer. As mentioned, the prediction precision of group 3, 4 and 5 are same, implying that there is no difference between employing the global and local geometry parameters as the input layer. The reason can be inferred that the weight of the irrelevant input parameters could automatically vanish during the training of the ANN. Therefore, in the following analysis, the global geometrical parameters of the film cooling arrangements are selected to construct the input layer and the regionally averaged temperature is chosen to form the output layer.

**Table 3** Some representative experiments with different inputs, outputs and the calculated number of hidden layer nodes corresponding to each ANN.

Group No.	1	2	3
Inputs	Global parameters 23	Global parameters 23	Global parameters 23
Outputs	Mean temperature of the blade surface $T_{sa1}$	Mean temperature of the leading edge $T_{sa2}$	Mean temperature of a Z-direction line on the pressure side $T_{la1}$
Nodes	9	9	9
Group No.	4	5	6
Inputs	Parameters of 3 columns around the line 11	Parameters of 1 column upstream of the line 5	Global parameters 23
Outputs	Mean temperature of the line $T_{la2}$	Mean temperature of the line $T_{la3}$	Mean adiabatic cooling efficiency of the line $\eta_a$
Nodes	7	5	9

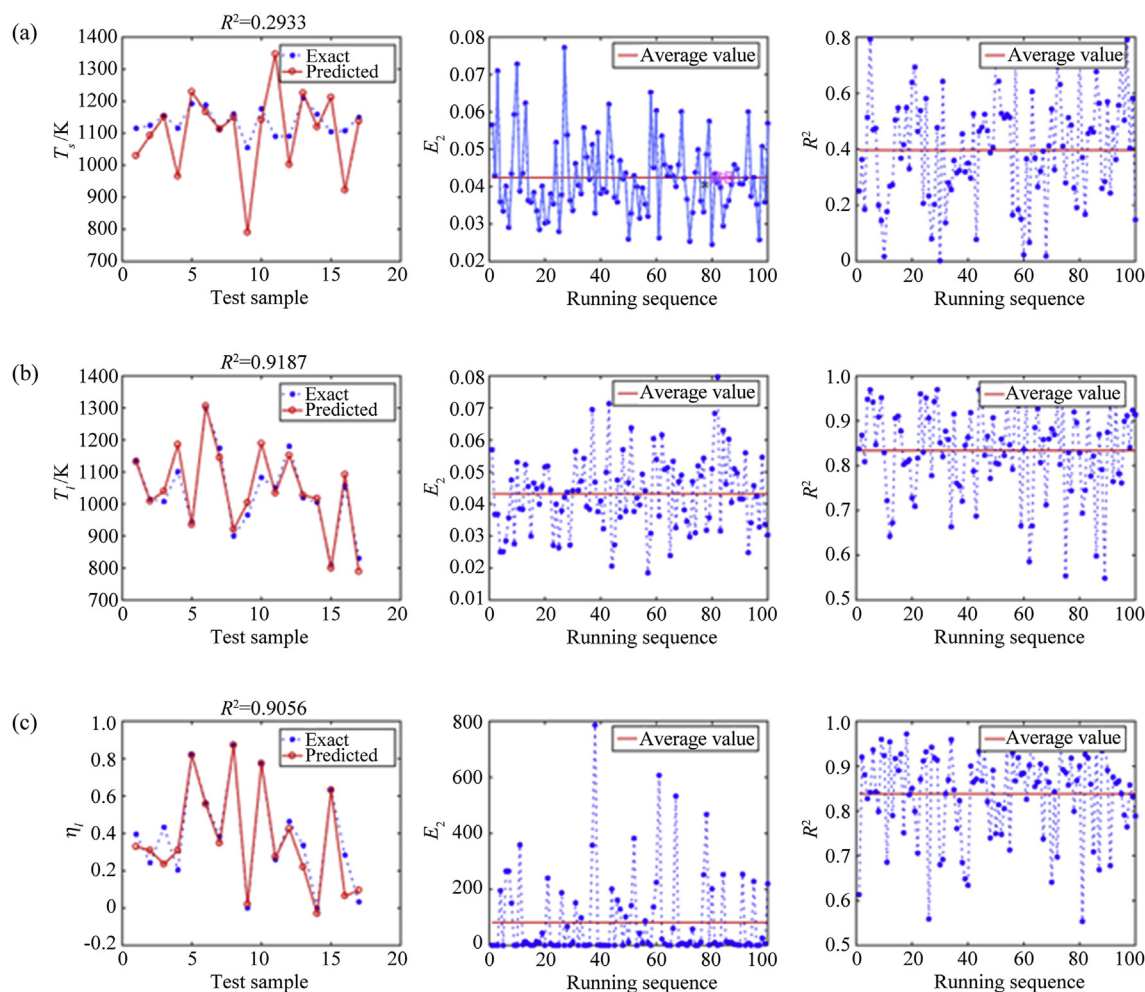


**Figure 5** The predicted temperature, mean relative error and fitting determination coefficient of (a) Group 1, (b) Group 3, (c) Group 6, with different inputs, outputs and hidden layer nodes.

### 3.1.2. Effect of ANN structure and activation function selection

Aside from the input and output layers, the number of the hidden layers, the number of nodes in each hidden layer, and the activation functions can also influence the prediction precision of the ANN. In the ANN, the relation between two connected neurons is described by an activation function. In general, the role of activation function is to introduce nonlinear factors into signal calculation to enhance the approximation ability of the network. Without activation function, no matter how many layers are there in the neural

network, the final output is still a linear combination of the initial input, which is equivalent to the absence of the hidden layers. Therefore, the structure and activation functions of the ANN were adjusted and some test results are shown in Table 4.

According to the comparison shown in Table 4, it can be seen that the single-hidden-layer ANN with 9 hidden layers and the ‘logsig-purelin’ activation function has the best performance. In general, the mean error does not vary too much from case to case, thus it is difficult to determine which one is superior. The results may be different if the dataset is rich enough.

**Table 4** Comparison of the test results with adjustments for the ANN structures and activation functions.

Structure	Activation function	Average $R^2$ for 100 runs	Highest $R^2$ in 100 runs	Average relative error for 100 runs
23-9-1	tansig-purelin	0.8143	0.95	4.75%
23-9-1	tansig-tansig	0.7362	0.98	5.87%
23-9-1	logsig-purelin	0.8227	0.97	4.41%
23-9-1	logsig-tansig	0.7944	0.95	5.09%
23-5-5-1	logsig-purelin	0.77	0.92	5.89%
23-7-7-1	logsig-purelin	0.7456	0.92	6.11%
23-9-7-1	logsig-purelin	0.7667	0.93	6.02%

### 3.1.3. Effect of introducing GA optimization

In addition to the above effects, the weights and biases of the neuron are another two important factors to the prediction accuracy and convergence speed of the ANN, which are updating during the training. Normally, the initial weights and biases are randomly generated so that the training process can start. However, when it comes to complex problems, the random initialization of weights and biases could lead to the convergence of the cost function to local minimum values, which may result in poor prediction accuracy. A useful optimization method for this is to introducing GA to find the optimal initial weights and biases of the network. With the same input, output and other conditions, the GA algorithm was introduced to optimize the ANN. The results are shown in Figure 6.

It can be seen that the performance of ANN is promoted by adopting the GA to optimize, but the improvement is not very obvious. From the tracking data during the program operation, after about 80 generations, the average fitness value of each generation of the population is equal to the optimal individual's, meaning that the population evolution has reached the highest level. Therefore, it is safe to conclude that the GA has already found the best individual. It is inferred that the poor performance of GA in this problem is induced by the tiny size of the ANN and the small amount of training data. Once the problem is more complex and the dataset is more abundant, the GA optimization could be necessary.

### 3.2. Multi-output ANN construction

As mentioned above, it is better to construct the output layer with the local parameters rather than the general parameters. Therefore, as shown in Figure 7, twenty sampling lines are arranged along the surface, where the local mean temperatures are calculated. In the previous ANNs, there is only one parameter in output layer. In order to predict the local mean temperature at these 20 sampling locations, it is required to construct an ANN with 20 parameters in the output layer. The results are shown in Figure 8. In general, all the predicted local mean temperature of the lines agrees well with the data from the CFD simulation. It is also found that increasing the number of hidden layers does not

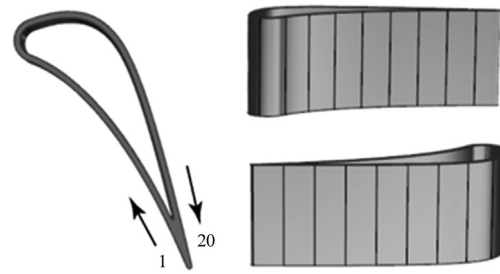


Figure 7 The geometric model of the guide vane which is divided into 20 equal parts along the surface.

influence the prediction precision too much due to the small dataset and relatively simple problem. The twenty-line sampling is a demonstration of the prediction ability of multi-output ANN. It is possible to arrange more sampling lines so that the temperature distribution along the turbine guide vane or along the vane height can be well resolved.

However, we found that the training process of these multi-output ANNs always stops because of the validation check rather than the MSE index mentioned in section 2.3. Validation check means that before training, the system randomly extracts some data as a validation set to monitor the change of generalization ability of the network in training. It needs a preset value which is 6 by default in MATLAB, which means that if the network does not reduce the prediction error of the validation set six consecutive times during the training, the prediction ability is considered not to increase any more, thus the training stops. This preset value can be artificially changed, but it needs to be adjusted within a reasonable range according to the complexity of the problem being studied. Too small will limit the training and hinder the ability improvement of the network. If it is too large, it will be tantamount to self-deception and waste computing resources, without better performance.

Trying to explain this problem in current work, we have to check these multi-output ANNs' performance on training set, test set and verification set, respectively. Therefore, we have drawn many regression images of the datasets in cases stopped by validation check. Most of them are very similar, as shown in Figure 9. The correlation coefficient  $R$  of the training set at the upper left position in Figure 9 is high, while of the validation set at the upper right and of the test

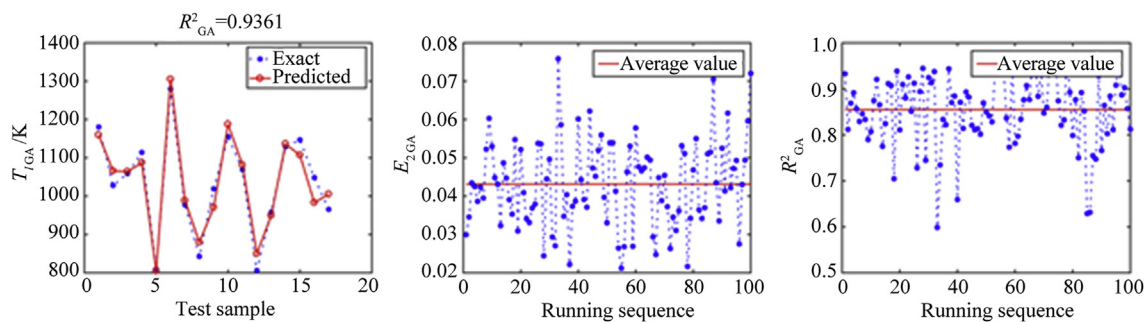
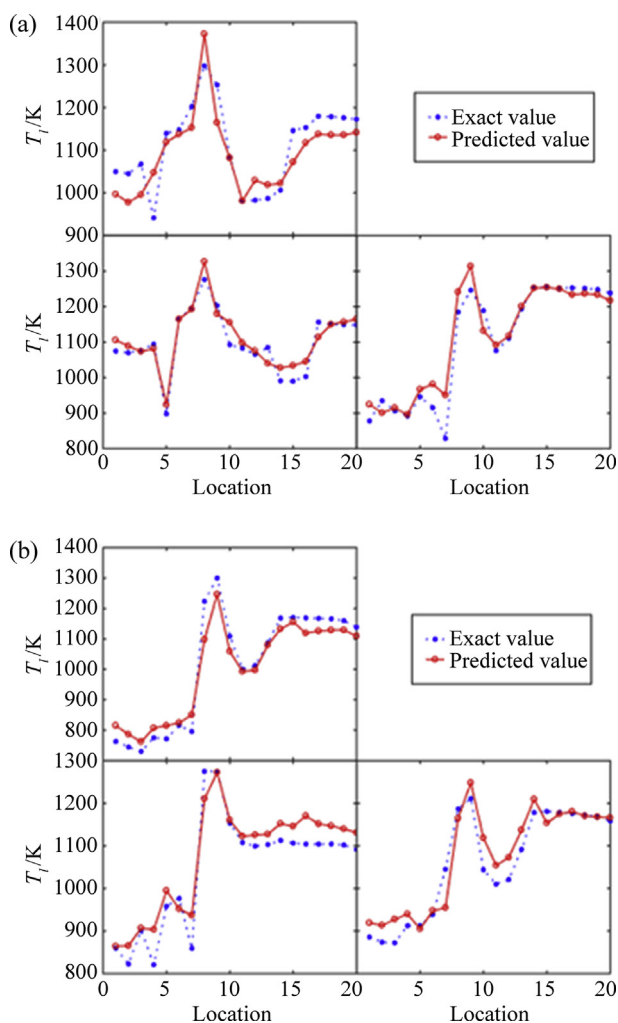


Figure 6 The predicted temperature, mean relative error and fitting determination coefficient of the test sets by introducing GA to optimize the ANN.





**Figure 8** The mean temperature prediction of the 20 lines along the vane surface for randomly three samples in the test set based on the ANN with (a) single-hidden-layer, (b) double-hidden-layers.

set at the lower left are significantly lower. In other words, the network has a better performance on the training set than other two sets, which means the prediction ability to new data is poor. That is called over-fitting. The reason for this may be that the structure of the network is relatively complicated after the number of outputs becomes 20, while the amount of data does not increase. From this, we can reasonably infer that when the data set is further expanded, the training process of the multi-output ANN can eventually stop by MES reducing to target value, rather than validation check. Thus, it is considered that the prediction precision of the multi-output ANN can be further improved.

### 3.3. Temperature distribution prediction tool development

Based on the abovementioned work, the trained ANN is able to make instantaneous prediction of the temperature variations of the guide vane based on the information of the

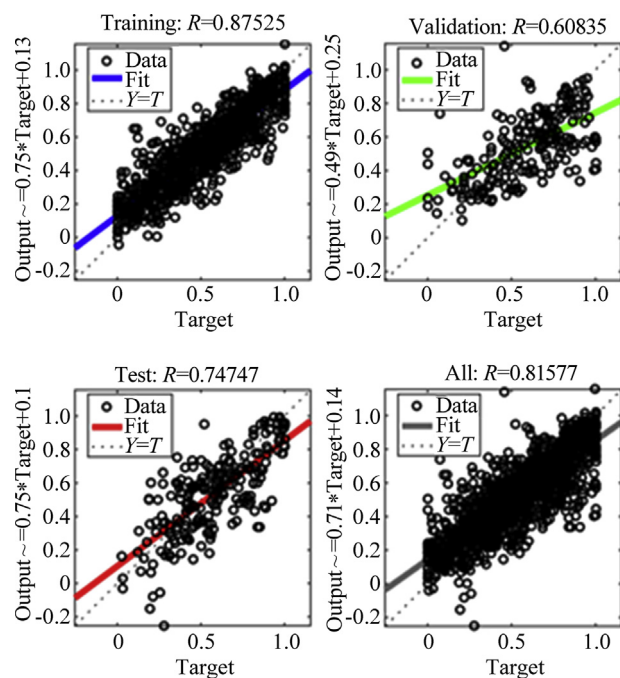


**Figure 9** The regression coefficients of the training set (upper left), the test set (lower left) and the verification set (upper right), and all the data sets together (lower right) for one of the cases to check the over-fitting.

arrangements of the film holes, such as location, diameter, inclination, etc. Due to fast prediction natural, this could be a very useful tool in the preliminary conceptual design of the cooling scheme of a guide vane. Therefore, a toolbox software is developed based on Python embedded with the multi-output ANN. With the GUI (graphical user interface), the designers can manually input or modify the parameters, import existing samples, and adjust the location and inclination of each array of the film holes by directly dragging on the image. The real time prediction of the surface temperature distribution across the guide vane can be made and displayed and all of the functions are implemented by self-written codes. It could facilitate the turbine designer to work out an initial design with high efficiency for the further local optimizations.

## 4. Conclusions

The main purpose of this work is to explore the method of machine learning to predict the cooling effectiveness on an entire 3-D guide vane from geometrical parameters of film cooling structure with high speed and precision, thus optimizing the turbine design process in the initial stage with AI technology. Based on the dataset obtained from massive simulation automation, the constructed ANNs were trained and tested, and many influencing factors were investigated and evaluated. The main conclusions are as follows.

- (1) The local parameters are better than the overall parameters to construct the output layer, with the determination coefficient between 0.8 and 0.95 and the relative error less than 5% in predicting temperature. However, there is no much difference in the results with different structures of the input layer.
- (2) The effects of the number of the hidden layers, the nodes in each hidden layer, the activation function selection, and the GA optimization are not obvious because the problem in this scenario is relatively simple and the training dataset is small.
- (3) The prediction of temperature distribution across the entire vane surface is realized through a multi-output ANN, and a prediction tool is developed based on it, having preliminarily achieved the AI aided design for the film cooling structure.

## Acknowledgements

The authors gratefully acknowledge funding support from the Program for National Natural Science Foundation of China (51876005).

## References

- [1] L. Jaw, Neural network modeling of engine tip clearance, in: 33rd Joint Propulsion Conference & Exhibit, Seattle, WA, 6-9 July, 1997, Paper No. AIAA 97-2775, <https://doi.org/10.2514/6.1997-2775>.
- [2] M. Cifaldi, N. Chokani, Engine monitoring using neural networks, in: 34th AIAA/ASME/SAE/ASEE Joint Propulsion Conference & Exhibit, 1998, Paper No. AIAA-98-3548, <https://doi.org/10.2514/6.1998-3548>.
- [3] Q.G. Zheng, C.W. Jin, Z.Z. Hu, H.B. Zhang, A study of aero-engine control method based on deep reinforcement learning, *IEEE Access* 7 (2019) 55285–55289, <https://doi.org/10.1109/ACCESS.2018.2883997>.
- [4] Z.N.S. Vanini, K. Khorasani, N. Meskin, Fault detection and isolation of a dual spool gas turbine engine using dynamic neural networks and multiple model approach, *Inf. Sci.* 259 (2014) 234–251, <https://doi.org/10.1016/j.ins.2013.05.032>.
- [5] J. Johnson, P. King, J. Clark, M. Ooten, Design optimization methods for improving HPT vane pressure side cooling properties using genetic algorithms and efficient CFD, in: 50th AIAA Aerospace Sciences Meeting Including the New Horizons Forum & Aerospace Exposition, Nashville, Tennessee, 09-12 January, 2012, Paper No. AIAA 2012-0326, <https://doi.org/10.2514/6.2012-326>.
- [6] A. Mousavi, S. Nadarajah, Adjoint-based multidisciplinary design optimization of cooled gas turbine blades, in: 51th AIAA Aerospace Sciences Meeting Including the New Horizons Forum & Aerospace Exposition, Orlando, Florida, 4-7 January, 2011, Paper No. AIAA 2011-1131, <https://doi.org/10.2514/6.2011-1131>.
- [7] C. Sotgiu, B. Weigand, K. Semmler, A turbulent heat flux prediction framework based on tensor representation theory and machine learning, *Int. Commun. Heat Mass Tran.* 95 (2018) 74–79, <https://doi.org/10.1016/j.icheatmasstransfer.2018.04.005>.
- [8] C.H. Wang, J.Z. Zhang, J.H. Zhou, Data mining optimization of laidback fan-shaped hole to improve film cooling performance, *J. Cent. S. Univ.* 24 (5) (2017) 1183–1189, <https://doi.org/10.1007/s11771-017-3521-x>.
- [9] C.H. Wang, J.Z. Zhang, J.H. Zhou, S.A. Alting, Prediction of film-cooling effectiveness based on support vector machine, *Appl. Therm. Eng.* 84 (5) (2015) 82–93, <https://doi.org/10.1016/j.applthermaleng.2015.03.024>.
- [10] K.D. Lee, S.M. Kim, K.Y. Kim, Numerical analysis of film-cooling performance and optimization for a novel shaped film-cooling hole, in: Proceedings of ASME Turbo Expo, Copenhagen, Denmark, 11-15 June, 2012, Paper No. GT2012-68529, <https://doi.org/10.1115/gt2012-68529>.
- [11] Y.M. Qin, X.Y. Li, J. Ren, H.D. Jiang, Prediction of the adiabatic film cooling effectiveness influenced by multi parameters based on BP neural network, *J. Eng. Thermophys.* 32 (2011) 1127–1130.
- [12] S. Dolati, N. Amanifard, H.M. Deylami, Numerical study and GMDH-type neural networks modeling of plasma actuator effects on the film cooling over a flat plate, *Appl. Therm. Eng.* 123 (2017) 734–745, <https://doi.org/10.1016/j.applthermaleng.2017.05.149>.
- [13] M. Naghashnejad, N. Amanifard, H.M. Deylami, A predictive model based on a 3-D computational approach for film cooling effectiveness over a flat plate using GMDH-type neural networks, *Heat Mass Tran.* 50 (2014) 139–149, <https://doi.org/10.1007/s00231-013-1239-3>.
- [14] K.D. Lee, D.W. Choi, K.Y. Kim, Optimization of ejection angles of double-jet film-cooling holes using RBNN model, *Int. J. Therm. Sci.* 73 (2013) 69–78, <https://doi.org/10.1016/j.ijthermalsci.2013.05.015>.
- [15] P.M. Milani, J. Ling, G. Saez-Mischlich, J. Bodart, J.K. Eaton, A machine learning approach for determining the turbulent diffusivity in film cooling flows, *ASME J. Turbo.* 140 (2) (2017) 2–14, <https://doi.org/10.1115/1.4038275>.
- [16] J.O. Davalos, J.C. Garcia, G. Urquiza, A. Huicochea, O. De Santiago, Prediction of film cooling effectiveness on a gas turbine blade leading edge using ANN and CFD, *Int. J. Turbo Jet Engines* 35 (2) (2016) 101–111, <https://doi.org/10.1515/tjj-2016-0034>.
- [17] M. Payandehdoost, N. Amanifard, M. Naghashnejad, H.M. Deylami, Robust model for predicting the average film cooling heat transfer coefficient over a turbine blade based on the finite volume study, *Heat Tran. Res.* 45 (7) (2014) 643–657, <https://doi.org/10.1615/Heat-TransRes.2014007180>.
- [18] P.M. Milani, J. Ling, J.K. Eaton, Physical interpretation of machine learning models applied to film cooling flows, *ASME J. Turbo.* 141 (1) (2018) 10–22, <https://doi.org/10.1115/1.4041291>.
- [19] A.R. Mostofizadeh, M. Adami, M.H. Shahdad, Multi-objective optimization of 3-D film cooling configuration with thermal barrier coating in a high pressure vane based on CFD-ANN-GA loop, *J. Braz. Soc. Mech. Sci. Eng.* 40 (4) (2018) 211–226, <https://doi.org/10.1007/s40430-018-1145-1>.
- [20] C. El Ayoubi, W. Ghaly, I. Hassan, Aero-thermal shape optimization for the discrete film cooling of a turbine airfoil, in: Proceedings of the ASME 2015 International Mechanical Engineering Congress and Exposition, Houston, Texas, 13-19 November, 2015, Paper No. IMECE2015-51871, <https://doi.org/10.1115/IMECE2015-51871>.
- [21] Y. Huang, J.Z. Zhang, C.H. Wang, Shape-optimization of round-to-slot holes for improving film cooling effectiveness on a flat surface, *Heat Mass Tran.* 54 (2018) 1741–1754, <https://doi.org/10.1007/s00231-017-2272-4>.
- [22] J.C. García, J.O. Dávalos, G. Urquiza, S. Galván, A. Ochoa, J.A. Rodríguez, C. Ponce, Film cooling optimization on leading edge gas turbine blade using differential evolution, in: Proceedings of the Institution of Mechanical Engineers, Part G: Journal of Aerospace Engineering, 7 March, 2018, <https://doi.org/10.1177/0954410018760151>.
- [23] G.M. Laskowski1, A.K. Tolpadi, M.C. Ostrowski, Heat transfer predictions of film cooled stationary turbine airfoils, in: Proceedings of ASME Turbo Expo, Montreal, Canada, 14-17 May, 2007, Paper No. GT2007-27497, <https://doi.org/10.1115/GT2007-27497>.
- [24] Z. Liu, L. Ye, C.Y. Wang, Z.P. Feng, Numerical simulation on impingement and film composite cooling of blade leading edge model

- for gas turbine, *Appl. Therm. Eng.* 73 (2) (2014) 1432–1443, <https://doi.org/10.1016/j.applthermaleng.2014.05.060>.
- [25] D.E. Metzger, R.S. Bunker, Local heat transfer in internally cooled turbine airfoil leading edge regions, part I: impingement cooling without film coolant extraction, *ASME J. Turbo.* 112 (3) (1990) 451–458, <https://doi.org/10.1115/1.2927680>.
- [26] J. Maikell, D. Bogard, J. Piggush, A. Kohli, Experimental simulation of a film cooled turbine blade leading edge including thermal barrier coating effects, *ASME J. Turbo.* 133 (1) (2011), <https://doi.org/10.1115/1.4000537>, 011-014.
- [27] K. Hiroaki, Empirical studies on the speed of convergence of neural network training using genetic algorithms, in: *Proceeding of AAAI-90 Boston, 1990*.
- [28] W. Wang, J.M. Gao, L. Xu, X.J. Shi, Experimental study and prediction of film cooling effectiveness for a guide vane in heavy gas turbines, in: *Proceedings of the 15<sup>th</sup> International Heat Transfer Conference, Kyoto, Japan, 10-15 August, 2014*, Paper No. IHTC15-9965, <https://doi.org/10.13140/2.1.4056.7681>.